

Supporting Information for:

Photocleavage of Poly(methyl acrylate) with Centrally Located o-Nitrobenzyl Moiety: Influence of Environment on Kinetics

M. E. Lee, E. Gungor, A. M. Armani

1. Synthesis of Photocleavable PMA

An o-nitrobenzyl moiety was incorporated into a bifunctional ATRP initiator according to Scheme 1 (main text). The final product was verified using ^1H NMR and is shown in Figure S1. Peak shifts and integration ratios are as expected for the molecular structure and are indicated in the figure.

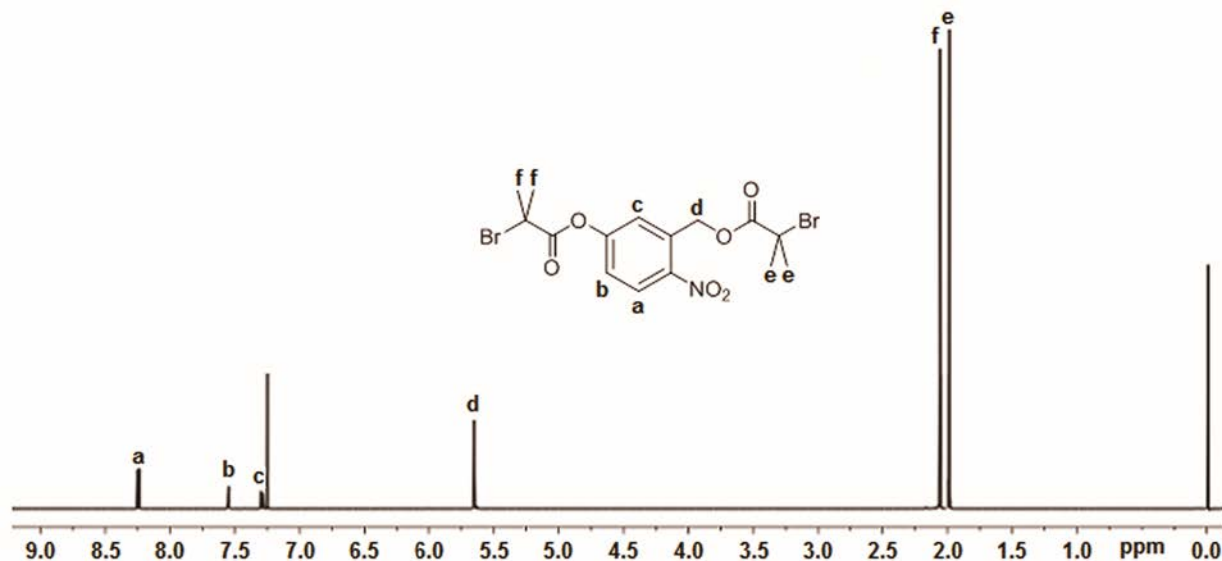


Figure S1. ^1H NMR spectrum of ONB bifunctional initiator in CDCl_3 .

Atom transfer radical polymerization (ATRP) was chosen as the polymerization method due to the high degree of control over chain growth rate¹. We were able to preserve narrow molecular weight distributions by terminating the reaction at early states of conversion (Table S1).

Table S1. Synthesis of Photocleavable PMA Prepared by ATRP.

Time (h) ^a	Conversion (mol %)	M_n , GPC ^b (g/mol)	M_w/M_n
0.583	19	11389	1.06
1	26	16215	1.05
1.5	31	20630	1.06
2.117	38	23571	1.09
4	53	32021	1.08
5	62	37620	1.08

^aATRP was carried out at 70 °C with a molar ratio $[\text{M}]_0:[\text{I}]_0:[\text{PMDETA}]_0:[\text{CuBr}]_0 = 800:1:2:2$, 10% (v/v) DMF. ^b GPC in THF calibrated with linear PS standards.

Figure S2 shows that the reaction possessed the kinetic characteristics of a controlled living radical polymerization¹. Namely, the log of change in monomer concentration was linear with time.

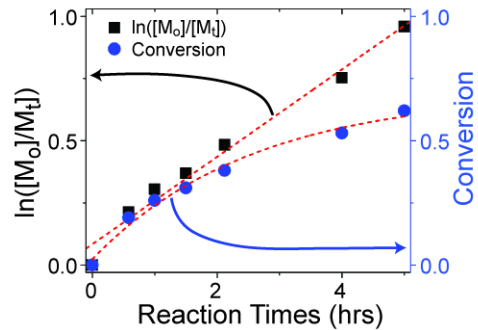


Figure S2. Kinetics of ATRP polymerization of methyl acrylate with ONB bifunctional initiator.

Resulting polymers were characterized using gel permeation chromatography (GPC) and ¹H NMR. The specific reaction times and molecular weight distributions for the polymers in Figure S2 are found in Table S1. The ¹H NMR peak shifts are as expected for the proposed PMA structure (Figure S3 and Figure S4).

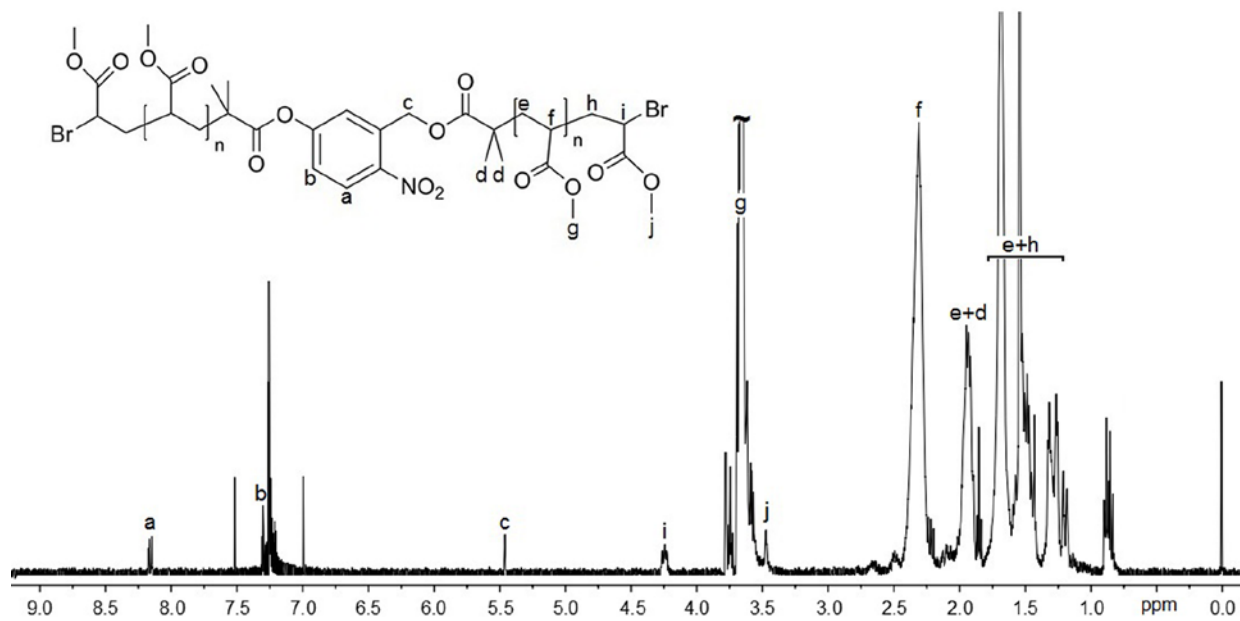


Figure S3. ^1H NMR spectrum of PMA containing a central ONB photocleavable group in CDCl_3 .

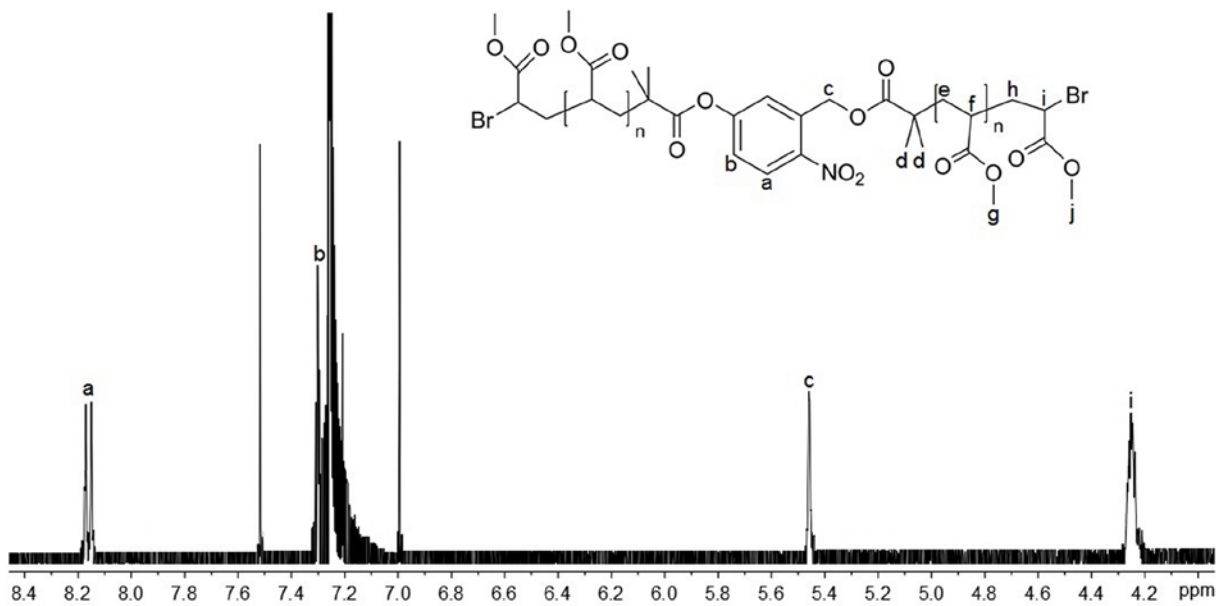


Figure S4. Expansion of the 8.5 to 4.0 ppm region of ^1H NMR spectrum of PMA containing ONB photocleavable group in CDCl_3 .

The initiator was synthesized and the polymerization reactions were repeated multiple times with $D < 1.10$ in order to generate sufficient quantities of the polymer to perform the kinetics measurements described in the manuscript. The distribution of the D values for all polymers is shown in Table S2.

Table S2: Summary of all polymers used in the present work.

Target M_n	M_n , GPC ^a (g/mol)	M_w/M_n
9000	8600	1.08
15000	14700	1.07
	14800	1.07
19000	19400	1.05
25000	24600	1.04
	24700	1.06
32000	32400	1.06
	30500	1.09

^a GPC in THF calibrated with linear PS standards

2. Analysis of cleaving behavior of polymers in film and in solution

a. UV-Vis Spectroscopy

The progress of photocleavage was monitored by tracking the change in the UV-Vis absorbance signal at 350nm with increasing amounts of UVA irradiation. The 25kDa polymer was used for this study. A subset of the UV-Vis spectra taken is shown in Figure S5.

As the photocleavage reaction progresses ($t = 0$ min to 320min), a broadening and an absorbance increase was observed between 300-350nm due to the formation of nitrosobenzaldehyde products. However, a signal decrease was observed at high exposure times ($t > 400$ min). This change in behavior is likely due to photo-dimerization of the nitrosobenzaldehyde photocleavage product. Similar effects have been observed previously², and

the mechanism is hypothesized to be a photoredox reaction of o-nitrosobenzaldehyde to form azobenzene bis(carboxylate), resulting in dimerization of adjacent chains³.

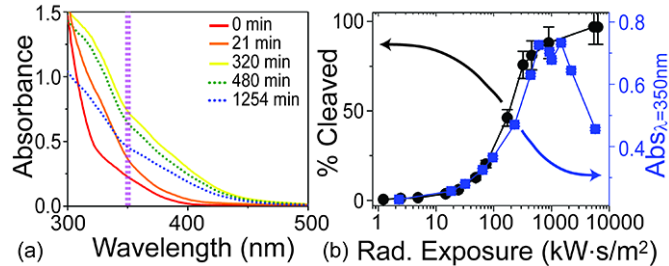


Figure S5. Comparison of GPC and UV-Vis analysis methods. a) UV-Vis spectra taken at several different UV exposure time points. As the photocleavage reaction of the 25k polymer progresses, the absorption in the 300nm-350nm region initially increases due to the formation of the nitrosobenzaldehyde. To compare these results with the GPC data, the absorption was calculated at 350nm (dashed purple line). b) Comparison between the GPC results (left y-axis) and UV-Vis measurements (blue axis). While the GPC results clearly show the entire photo-cleavage reaction, the UV-Vis are only able to capture the initial portion of the photocleavage behavior due to the formation of byproducts that interfere with the nitroso-group UV-Vis signal.

Therefore, while a majority of the photocleavage reaction occurs before the decrease in absorbance, we cannot accurately record the photoproduct formation at high UV exposure times. As a result, UV-Vis spectroscopy alone is not sufficient for monitoring the entire kinetic photocleavage process.

b. Kinetics results for all polymers

Figure S6 shows all of the kinetic curves for all of the polymers studied for this work. % cleaved was determined by dividing the GPC peak height at cleaved, low molecular weight by the total height of both GPC peaks. Note that secondary photo-initiated processes occurred in the

film at high UV doses, manifesting as an apparent decrease in percent cleaved (Figure S6d). These points are designated by hollow symbols. These values were not included in the fit. For the film samples, the fit was pinned to the maximum value achieved in a given reaction. All fits for solution samples were unconstrained.

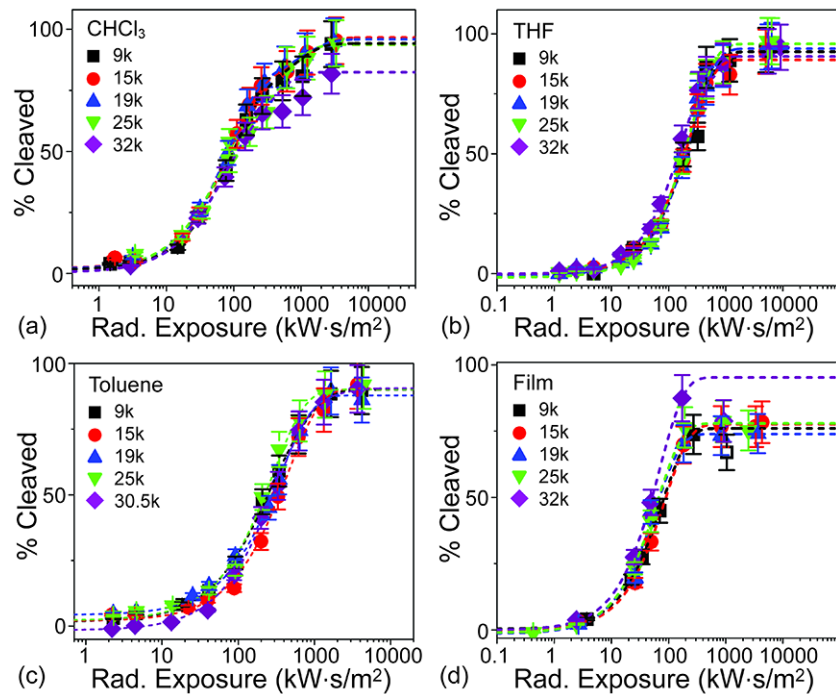


Figure S6. Photocleavage kinetics ($\lambda = 350\text{nm}$) of polymer dissolved in a) chloroform, b) THF, c) toluene and d) spin-coated onto silicon wafers as a thin film.

From these fits, we determined the kinetic rate constants for the reaction. However, it is important to note that the x-axis units are radiant exposure. Therefore, the rate constants are in units of $\text{m}^2/\text{kW}\cdot\text{s}$. As such, the rate constants determined from these fits are actually the intensity normalized rate constants or generalized rate constants which are independent of the specific experimental set-up. This can be formally expressed as:

$$k_{generalized} = \frac{k}{I_{avg}} = \frac{\phi \epsilon}{N_A h \nu} \quad (1)$$

where k is the rate constant of the system, I_{avg} is the average optical intensity, ϕ is the quantum efficiency, ϵ is the molar absorptivity (determined from UV-Vis data), N_A is Avagadro's number, h is Planck constant, and ν is the frequency of light (350nm).

Using the kinetic data found in Fig S6, we calculated the quantum efficiencies (ϕ) of each set of reaction conditions in solution. For consistency, reaction progress up to 50% cleaved was used in the analysis for all samples. By plotting the number of moles of photoproduct formed (as determined by GPC) against the number of incident photons, we determined the quantum efficiency of each reaction. The number of moles of photoproduct formed and incident photons can be described by the following equation:

$$\phi = \frac{m_{cleav}}{m_{phot}} = \frac{(RE)(A)/E_{350}}{(\%cleav)(m_{init})} \quad (2)$$

where RE is radiant exposure, A is exposure area, E_{350} is the energy of a 350nm photon, %cleav is the fraction of total polymer that has been cleaved, and m_{cleav} , m_{phot} , m_{init} are the number of moles of cleaved product, photons, and initial polymer respectively.

3. Control experiments

a. Dependence of rate constants on ONB concentration

In order for the proposed model to be accurate, it is important to operate in a regime where the reaction is not limited by the reactant availability. Otherwise, the rate constants become functions of the reactant concentration. In the present case, this regime corresponds to having an

excess of photons in relation to the number of ONB groups. A straightforward way to verify that the photon number is sufficiently high is to study the dependence of the rate constant on the ONB concentration.

This series of measurements was performed by varying the concentration of ONB group from 0.02mM to 1mM. We found that increasing the concentration to 1mM significantly changed the rate, indicating a breakdown in the model. However when the concentration is between 0.02mM and 0.3mM, little change was observed. Therefore, to retain enough sample for the GPC analysis with these results, we choose 0.3mM as the concentration for all experiments.

b. Effect of BHT on Photocleavage

A small amount of BHT was added to each solvent to serve as a hydrogen donor scavenger, inhibiting photodimerization during the photocleavage process⁴. When BHT was absent from the solution, GPC peaks corresponding to coupled o-nitrosobenzaldehyde photoreaction products were present early in the reaction (< 50% cleaved). However, in the presence of BHT, these peaks were greatly reduced. Because THF contains 250-350ppm of BHT as inhibitor, this solvent was unmodified. In the case of toluene and chloroform, BHT was added in 0.5wt% concentration. A control study was performed on the 25 kDa polymer in THF with 250ppm BHT and 0.5wt% BHT, and we found that any changes in the kinetic curve were within the error of the initial measurement.

c. Verification of wavelength specificity

As an additional control experiment, we observed the photocleavage reaction progress upon exposure to visible light using a fluorescent lamp. The first cleaved peaks occurred after 3 hours

of visible exposure. For reference, using the same molecular weight polymer with UV exposure, the first peaks appeared after 1 minute, and at 3 hours, nearly 85% of the polymer had cleaved. From these experiments, we concluded that minimal photocleavage occurs at wavelengths in the visible range.

SUPPLEMENTARY REFERENCES

1. Matyjaszewski, K.; Xia, J. H. *Chemical Reviews* **2001**, 101, (9), 2921-2990.
2. Chiantore, O.; Trossarelli, L.; Lazzari, M. *Polymer* **2000**, 41, (5), 1657-1668.
3. Zhou, H.; Lu, Y.; Qiu, H.; Guerin, G.; Manners, I.; Winnik, M. A. *Macromolecules* **2015**, 48, (7), 2254-2262.
4. Fujisawa, S.; Kadoma, Y.; Yokoe, I. *Chem Phys Lipids* **2004**, 130, (2), 189-195.